

# Numerical Modeling on Thermal Loading of Diamond Crystal in X-ray FEL Oscillator <sup>\*</sup>

SONG Mei-Qi() <sup>1</sup>   ZHANG Qing-Min () <sup>1,1)</sup>   GUO Yu-Hang () <sup>1</sup>  
 LI Kai () <sup>2</sup>   DENG Hai-Xiao() <sup>2</sup>

<sup>1</sup> Department of Nuclear Science and Technology, School of Energy and Power Engineering,  
 Xian Jiaotong University, Xian 710049, China

<sup>2</sup> Shanghai Institute of Applied Physics, Chinese Academy of Sciences, Shanghai 201800, China

**Abstract:** Due to high reflectivity and high resolution to X-ray pulse, diamond is one of the most popular Bragg crystals serving as the reflecting mirror and mono-chromator in the next generation free electrons lasers (FELs). The energy deposition of X-rays will result in thermal heating, and thus lattice expanding of diamond crystal, which may degrade the performance of X-ray FELs. In this paper, the thermal loading effect of diamond crystal for X-ray FEL oscillator has been systematically studied by the combined simulation of Geant4 and ANSYS, and its dependence on the environment temperature, crystal size, X-ray pulse repetition rate and pulse energy are presented.

**Key words:** X-ray pulse, diamond crystal, energy deposition, X-ray FEL oscillator,

**PACS:** 41.60.Cr

## 1 Introduction

Driven by the successful operation of the hard X-ray free-electron lasers (FELs) [1, 2] and the growing interests of scientific users, several hard X-ray FEL facilities are being constructed and planned around the world. Currently, all these FELs use self-amplified spontaneous emission (SASE) [3] as the lasing mode for the hard X-ray, which starts from the beam noise, and results in radiation with transverse coherence, but poor longitudinal coherence. Therefore, various seeded FEL schemes were intensively studied [4–6] worldwide to generate fully coherent FEL radiation, especially in the soft X-ray regime.

In the hard X-ray regime, with the development of high-reflectivity and high-resolution crystal, alternative fully coherent FEL schemes are proposed and of great interest. On one hand, the self-seeding approach has been experimentally demonstrated to narrow the SASE bandwidth [7, 8]. In a self-seeding scheme, the noisy SASE radiation generated in the first undulator section is spectrally purified by a crystal filter. Then, in the second undulator section, this spectrally purified FEL pulse serves as a highly coherent seed to interact with the electron bunch again to configure a FEL amplifier, which could significantly improve the temporal coherence of the final output radiation. On the other hand, the low-gain oscil-

lator has been reconsidered as a promising candidate for a hard X-ray FEL through the use of X-ray crystal cavity, known as XFEL [9–12]. It is widely believed that with the peak brilliance comparable to SASE and the average brilliance several orders of magnitude higher than SASE, XFEL may open up new scientific opportunities in various research fields.

In these next generation FELs, the interaction between X-ray FEL pulse and crystal can cause energy deposition in crystal and results in the raising of crystal temperature, further expanding of crystal volume and lattice. Hence, the Bragg energy would be shifted and the reflection spectrum would be enlarged, which is called as thermal loading effect of X-rays and is not negligible because of high brightness of X-ray pulse. In this paper, we numerically investigate the interaction between X-ray pulse and diamond crystal in XFEL by using Geant4 [13] and its thermal conduction through ANSYS [14]. In section 2, the numerical model, the general result of energy deposition and temperature raise are described. The thermal loading dependences on the environment temperature, crystal size, X-ray repetition rate and pulse energy are illustrated and discussed in section 3. Finally, we summarize the optimal parameters of diamond crystal and X-ray pulse in the conclusions.

Received 13 October 2015

<sup>\*</sup> Supported by National Natural Science Foundation of China (11175240, 11205234, 11322550) and Program for Changjiang Scholars and Innovative Research Team in University (IRT1280)

1) E-mail: zhangqingmin@mail.xjtu.edu.cn

©2013 Chinese Physical Society and the Institute of High Energy Physics of the Chinese Academy of Sciences and the Institute of Modern Physics of the Chinese Academy of Sciences and IOP Publishing Ltd.

## 2 Numerical Modeling

To study the thermal loading effects, in this section, the interactions between incident X-ray photon pulse and diamond crystal are modeled using Geant4 firstly to get the photon energy deposition and thermal conversion. Then the collected data are imported to ANSYS to investigate the temperature shift of the crystal during the penetration of X-ray pulse.

According to the early theoretical results of XFELO [8–12], a set of baseline parameters are assumed for the X-ray pulses here. X-ray photon energy is 12.04keV, with  $n = 1 \times 10^{10}$  photons per pulse and 1MHz repetition rate. In the longitudinal dimension, X-ray pulse is supposed to be uniformly distributed within a time window of  $\tau = 0.5\text{ps}$ , while a Gaussian distribution with RMS size of  $65\mu\text{m}$  in the transverse direction. For the diamond crystal, the transverse region of interest is  $1\text{mm} \times 1\text{mm}$ , and the thickness is  $200\mu\text{m}$ .

In order to simplify description, we define a coordinate system  $(x, y, z)$ , with x-axis and y-axis parallel to crystal surface while z-axis perpendicular to it. And the X-ray photon pulse propagates in z-axis. In Geant4 setup, the outer of detector is air ( $2\text{mm} \times 2\text{mm} \times 0.6\text{mm}$ ), while the inside is carbon atom which is set as sensitive detector ( $1\text{mm} \times 1\text{mm} \times 0.2\text{mm}$ ). When X-ray energy deposition happened in the sensitive detector, the deposition location and the deposition amplitude are recorded. In our simulation, the X-ray intensity is acquired by applying Gaussian sampling along x and y axis. And only the Photoelectric effect and Compton scattering effects are concerned, because the incident photon energy is 12.04keV which is far less than the threshold 1.02MeV of electron pair effect.

The X-ray energy deposition distribution function  $\Delta E(x, y, z)$  can be obtained by summing up the energy deposition happened in the given small volume  $\Delta V$ . Then the converted thermal power distribution during the duration of X-ray pulse is given by

$$h(x, y, z, t) = \frac{\Delta E(x, y, z)}{\tau \Delta V} \frac{n}{N_e} (1 - R) \quad (1)$$

where  $N_e$  is the number of the total simulated events in the Geant4,  $R$  is the X-ray reflectivity of diamond crystal.

If we consider an X-ray pulse propagates through a 50mm-thick crystal which is sufficient to absorb almost all photons. As demonstrated in Fig. 1, the energy deposition decreases exponentially with the depth of crystal. In further studies with the secondary electrons taken into account, a raising up at the initial hundreds of nanometers exists [15, 16], which is invisible here, because it's

significantly small compared to the thickness of crystal. In practice, the thickness of diamond crystal is usually hundreds of micrometers (taken  $200\mu\text{m}$ ), and thus the X-ray energy deposition dependence on the crystal thickness can be ignored as shown in the subfigure of Fig. 1.

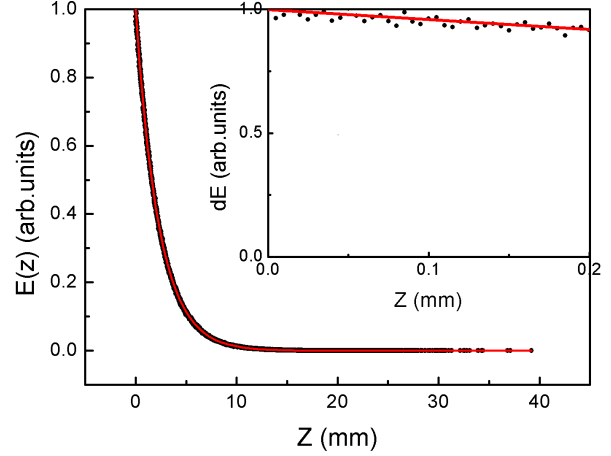


Fig. 1. X-ray energy deposition along the longitudinal direction within the crystal.

Fig. 2 shows the transverse X-ray energy deposition. With the ignorance of secondary electrons, it performs a Gaussian distribution, as shown in Fig. 2, which is an identical map to the power distribution of incident X-ray pulse.

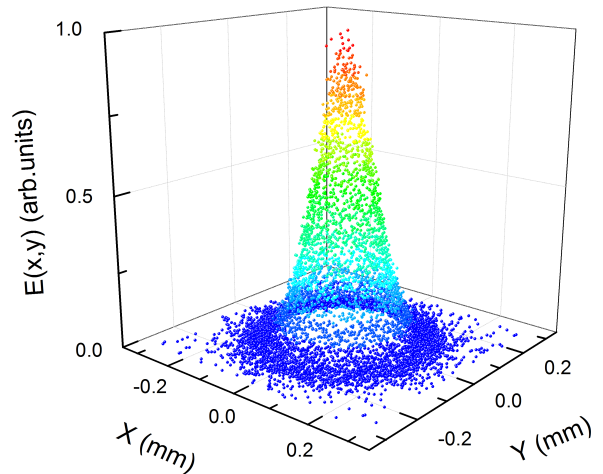


Fig. 2. X-ray energy deposition along the transverse direction of the crystal.

When an X-ray pulse containing of  $1 \times 10^{10}$  photons (nearly  $19.3\mu\text{J}$ ) is injected into a diamond crystal with the reflectivity of 90%, the thermal power distribution derived from simulation is written as

$$h(x, y, z, t) = \begin{cases} 5.296 \times 10^{16} e^{-\frac{x^2+y^2}{8.521 \times 10^{-9}}} e^{-436z} & (10^{-6}k \leq t \leq 10^{-6}k + 5 \times 10^{-13}) \\ 0 & (10^{-6}k + 5 \times 10^{-13} \leq t \leq 10^{-6}(k+1)) \end{cases} \quad (2)$$

Where  $k=0,1,2,\dots$ .  $x, y$  and  $z$  are in the unit of m,  $h$  is in  $\text{W}/\text{m}^3$  and  $t$  is in second. According to Eq. (2), nearly  $0.15\mu\text{J}$  X-ray photon energy will be absorbed in a  $200\mu\text{m}$  thick crystal.

In order to acquire the thermal behavior of diamond crystal under exposure of X-ray pulses, the heat source according to thermal power distribution Eq. (2) is imported into ANSYS to study the thermal transportation of diamond crystal. In ANSYS transient thermal analysis module, proper grid size and time-step are optimized for saving computer memory and calculating time, as well as ensuring the accuracy. For the  $0.5\text{ps}$  long X-ray pulse of  $1\text{MHz}$  repetition rate in our study, time-step of  $1 \times 10^{-13}\text{s}$  and  $2 \times 10^{-8}\text{s}$  are chosen for the temperature raise and heat dissipation process, respectively.

Under an environment temperature of  $300\text{K}$ , the temperature distribution at different position of the crystal was simulated. For a thin crystal here, the hottest location is the center of the crystal due to thermal conduction, which is the most important point that we should focus on in the following discussion. Fig. 3 presents one typical temperature change at the center of crystal. It is obvious that the temperature change consists of two items:  $\Delta T_1$  and  $\Delta T_2$ , which are contributed by the short-term heating due to X-ray photon energy deposition and long-term heating accumulation of remaining heat in the crystal, respectively.

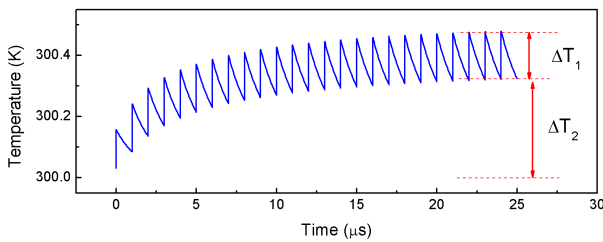


Fig. 3. Temperature changes at the crystal center under  $300\text{K}$  environment temperature.

### 3 Results and discussions

Both the user applications and the FEL buildup of an XFEL require spectral width less than  $1\text{meV}$  for X-ray pulse [17]. However, with temperature increasing, crystal volume expands as well as lattice spacing, which leads to shift of Bragg energy and broadening of XFEL bandwidth. According to the formula  $\Delta E/E = \beta \Delta T$  [18], there exists a critical temperature change  $\Delta T_c$  for diamond crystal to maintain the required X-ray bandwidth ( $<1\text{meV}$ ). As shown in Fig. 3, for an XFEL operation, both  $\Delta T_1$  from X-ray pulse energy deposition and

$\Delta T_2$  from remaining heat accumulation may degrade the buildup of XFEL from shot noise and the output stability after XFEL saturation. Thus a criterion of the total crystal temperature change  $\Delta T_t$  can be written as follows.

$$\Delta T_t = \Delta T_1 + \Delta T_2 < \Delta T_c \quad (3)$$

In this section, the heating dependence on the environment temperature, crystal size, X-ray pulse repetition rate and pulse energy are investigated.

#### 3.1 The environment temperature

To investigate the effect of environment temperature, we use the baseline parameters for X-ray and diamond crystal, while setting environment temperature as  $77\text{K}$ ,  $100\text{K}$ ,  $200\text{K}$  and  $300\text{K}$  respectively. After interaction with X-ray pulse in cold environment such as  $77\text{K}$  shown in Fig. 4, crystal temperature rises to a higher level and recovers more quickly than that at high temperature of  $300\text{K}$  (Fig. 3).

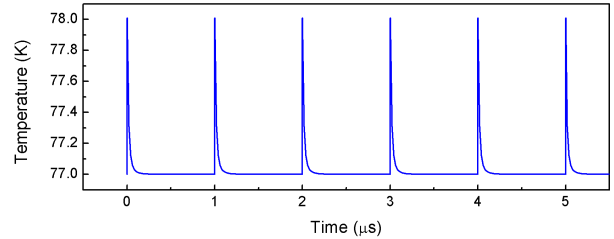


Fig. 4. Temperature changes at the crystal center under  $77\text{K}$  environment temperature.

The thermal conductivity  $\lambda$ , specific heat capacity  $C$ , and thermal expansion coefficient  $\beta$  of diamond crystal varies dramatically as the external temperature changes [19], as summarized in Table 1. Obviously, a lower environment temperature ensures higher thermal conductivity coefficient of diamond crystal, which guarantees heat losing quickly and crystal temperature being almost recovered before the arrival of the next X-ray pulse.

Table 1. The thermal parameters and the tolerated temperature shift of diamond crystal with the varying of environment temperature. [19]

T/K	77	100	200	300
$\lambda / \text{W}(\text{m} \cdot \text{K})^{-1}$	8973	7845	4129	2347
$C / \text{J}(\text{kg} \cdot \text{K})^{-1}$	7	15	122	410
$\beta / \text{K}^{-1} \times 10^{-8}$	3.4	7.4	60	120

Fig. 5 illustrates the crystal temperature changes at different environment temperature. As the external tem-

perature increases,  $\Delta T_1$  decreases and  $\Delta T_2$  increases because of independent behavior of the special heat capacity and thermal conductivity, respectively. Meanwhile  $\Delta T_i$  also shows a monotonous decrease after the competition of special heat capacity and thermal conductivity. For the baseline case discussed here, when the environment temperature is 77K, 100K and 200K, the total temperature shift  $\Delta T_t$  is lower than  $\Delta T_c$ . However,  $\Delta T_t$  at 300K is higher than its corresponding  $\Delta T_c$ , which means it can not be accepted.

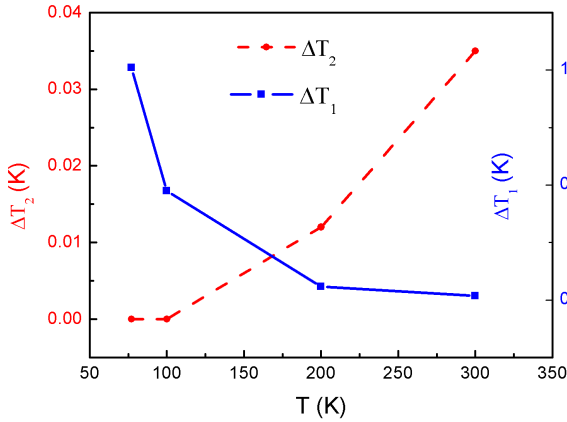
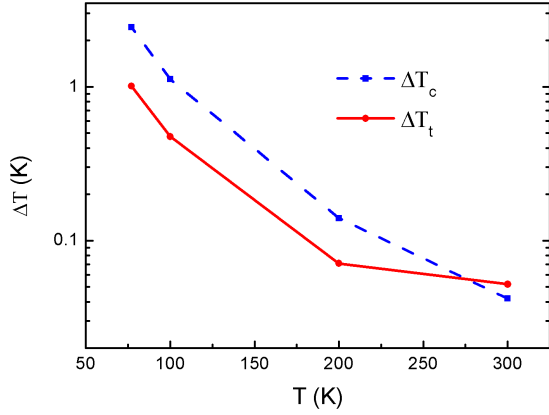


Fig. 5. Crystal temperature change with varying of environment temperature.

### 3.2 The crystal size

The size of diamond crystal contains two aspects: transverse cross section area and thickness. To begin with, we study the relation between crystal transverse cross section area and the temperature change at the center of crystal. The deposited heat is conducted outside mainly through the surface of a thin crystal, thus it is obvious that as the transverse area increase, the temperature shift is nearly constant as long as the cross section area is large enough to cover most of the incident X-ray photons. It agrees well with simulation results.

The influence of crystal thickness has been studied by applying heat source according to Eq. (2) to ANSYS

analysis. Taking different thickness of crystal in ANSYS and the simulation results are shown in Fig. 6. It is found that not only can the thinner mirror cool down faster, but also it can achieve a lower stable temperature. The reason is that the thinner the crystal is, the quicker it conducts heat to the environment.

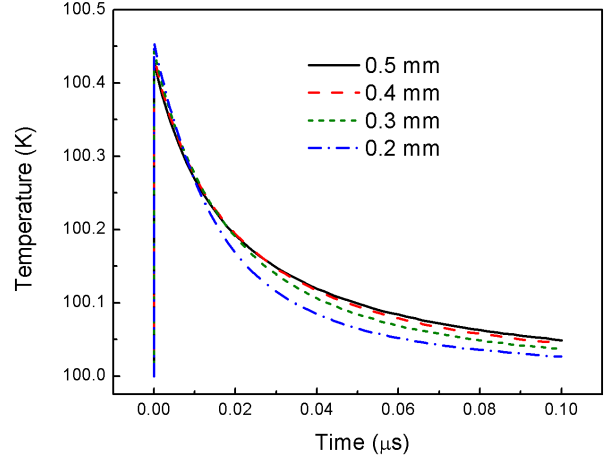


Fig. 6. The highest temperature change during cooling progress with varying crystal thickness.

For a 0.5mm thickness crystal, the temperature evolutions on longitudinal axis during the cooling progress are shown in Fig. 7. As time goes by, the highest temperature location moves towards the center of crystal. It is obvious that the influence of the crystal thickness on XFEL is more gently, compared to the environment temperature.

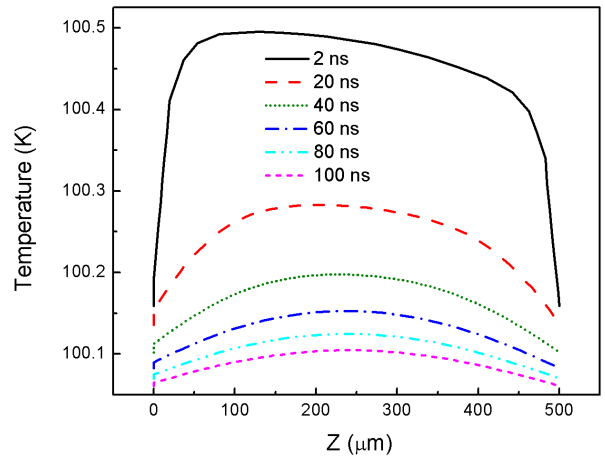


Fig. 7. Temperature changes on the crystal longitudinal axis, with the thickness of 0.5mm and environment temperature of 100K.

### 3.3 X-ray pulse repetition rate

To study the impact of the incident X-ray pulse repetition rate on the crystal temperature, we gradually increase the repetition rate from 1MHz to 80MHz for 100K

case. Maximum temperature as a function of X-ray repetition rate is shown in Fig. 8. With the repetition rate increase, the time duration for cooling process becomes short, which means that crystal temperature cannot fully recover before the arrival of next X-ray pulse, thus the temperature change  $\Delta T_2$  will raise because of residual heating accumulation. As mentioned in previous section, in order to keep the bandwidth less than 1meV, the highest temperature should be below 101.12K. Combined with the simulation results, the acceptable highest pulse repetition rate is 63.64 MHz, for the X-ray photon pulses assumed in section 2.

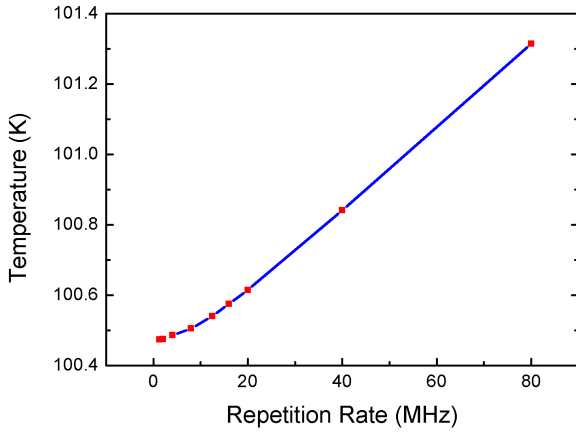


Fig. 8. The highest crystal temperature with different X-ray pulse repetition rate.

### 3.4 X-ray pulse energy

As mentioned above, the thermal loading of X-ray photon pulse is a function of photon flux and distribution, crystal reflectivity and thickness. It performs as a source providing heating energy to raise temperature. If  $1 \times 10^{10}$  photons are injected into a  $200 \mu\text{m}$  thick crystal,  $0.15 \mu\text{J}$  energy is absorbed under the conditions we have chosen. Because X-ray is so short and temperature increment is so little ( $< 5\text{K}$ ) that thermal conduction during heating process and heat capacity shift can be ignored, thus the highest crystal temperature is proportional to the amount of the incident X-ray pulse energy which is illustrated in Fig. 9. It's worth mention that for satisfying the energy bandwidth criterion ( $\Delta E < 1 \text{ meV}$ ), the X-ray pulse energy should be less than  $45 \mu\text{J}$ , under the environment temperature of 100K. It is worth stressing here that, the X-ray pulse energy in the cavity is  $43.5 \mu\text{J}$  for the original XFEL proposal operated at the fundamental of the resonant wavelength [9], while the typical photon pulse energy in the cavity is  $3.4 \mu\text{J}$  for a harmonic lasing scheme of XFEL [12], which is proposed to cut down the size and cost of large-scale machines.

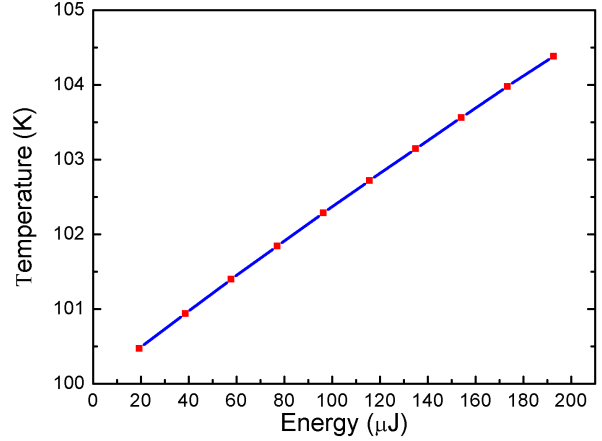


Fig. 9. The highest crystal temperature with different X-ray pulse energy.

## 4 Conclusions

Diamond crystal is commonly accepted as the material for fabricating mirrors for X-ray FEL oscillator. One of the most critical question still open is that how the thermal loading of diamond crystal degrade the performance of X-ray source. In this paper, Geant4 and ANSYS are jointly used to simulate the interaction between X-ray photon pulse and diamond crystal, and the crystal temperature shift due to thermal loading. Our results indicate that, a diamond crystal with large transverse cross section and small thickness, and a low environment temperature is helpful to relax the thermal loading effects in XFEL. For the XFEL example operated at 1MHz repetition rate in this paper, in order to ensure the bandwidth of 1meV, the X-ray pulse energy in the Bragg cavity should be lower than  $45 \mu\text{J}$  under 100K environment temperature.

It is expected that this result is useful for the manufacture and establishment of a feasible crystal mirror in X-ray FEL oscillator. It is worth stressing that this study is preliminary and there are still several practical physical effects that are not included, such as the accurate calculation of crystal reflectivity from dynamic theory [20], the noisy start-up and coherent build-up of XFEL, and the thermal expansion of the crystal lattice. These and other effects will be left for our subsequent reports. The numerical method used here can be easily extended to model the mono-chromator in the hard X-ray FEL self-seeding schemes.

*The authors would like to thank Shuaishuai Shen, Bo Liu and Dong Wang for helpful discussions.*

## References

- 1 Emma P et al. Nature Photon, 2010, 4: 641.
- 2 Ishikawa T et al. Nature Photon, 2012, 6: 540.
- 3 Bonifacio R et al. Opt. Commun., 1984, 50: 373.
- 4 YU L H. Phys. Rev. A, 1991, 44: 5178.
- 5 Stupakov G. Phys. Rev. Lett., 2009, 102: 074801.
- 6 DENG H, FENG C. Phys. Rev. Lett., 2013, 111: 084801.
- 7 Amann J et al. Nature Photon, 2012, 6: 693.
- 8 Ratner D et al. Phys. Rev. Lett., 2015, 114: 054801.
- 9 Kim K J et al. Phys. Rev. Lett., 2008, 100: 244802.
- 10 Shvydko Y et al. Nature Phys, 2010, 6: 196.
- 11 Lindberg R et al. Phys. Rev. ST Accel. Beams, 2011, 14: 010701.
- 12 DAI J, DENG H, DAI Z. Phys. Rev. Lett., 2012, 108: 034802.
- 13 Geant4 Working Group. Geant4 Manual.
- 14 Manual A U. ANSYS Users Manual. SAS IP inc, 1998.
- 15 Fundamental of Radiation Protection. (Atomic Energy Press, Beijing, 1982).
- 16 ZHONG H, CHANG W, ZHANG F et al. Chinese Medical Physics Magazine, 1996, (3).
- 17 Kim K J, Shvydko Y V. Phys. Rev. ST Accel. Beams, 2009, 12(3): 030703.
- 18 Stoupin S et al. Phys. Rev. Lett., 2010, 104: 085901.
- 19 Solid State Physics. (Tsinghua University Press, Beijing, 1989).
- 20 Shvydko Y, X-Ray Optics: High Energy Resolution Applications (Springer, Berlin, 2003).